Oxide-Induced Crack Closure: An Explanation for Near-Threshold Corrosion Fatigue Crack Growth Behavior

S. SURESH, G. F. ZAMISKI, AND R. O. RITCHIE

The concept of oxide-induced crack closure is utilized to explain the role of gaseous and aqueous environments on corrosion fatigue crack propagation *at ultralow, near-threshold growth rates* in bainitic and martensitic 2 ¼ Cr-1 Mo pressure vessel steels. It is shown that at low load ratios, near-threshold growth rates are significantly reduced in moist environments (such as air or water), compared to dry environments (such as hydrogen or helium gas), due to the formation of excess corrosion deposits on crack faces which enhances crack closure. Using Auger spectroscopy, it is found that at the threshold stress intensity, ΔK_o, below which cracks appear dormant, the maximum thickness of excess oxide debris within the crack is comparable with the pulsating crack tip opening displacement. The implications of this model to near-threshold fatigue crack growth behavior, in terms of the role of load ratio, environment, and microstructure are discussed.

DESCRIPTIONS of the environmental contributions to cracking during stress corrosion and corrosion fatigue have traditionally involved mechanisms generally classified in terms of hydrogen embrittlement or active path corrosion (*i.e.* metal dissolution) processes.[1] At very low growth rates ($<10^{-6}$mm/cycle) in fatigue, however, approaching the so-called threshold stress intensity ΔK_o for no detectabale crack growth, recent studies[2-5] in steels have indicated corrosion fatigue behavior totally inconsistent with such mechanisms. For example, environmentally-affected *near-threshold* fatigue crack growth has been found a) to predominate only at low load ratios,[2-5]* b) to be markedly *accelerated*

*Load ratio is defined as $R = K_{min}/K_{max}$ where K_{max} and K_{min} are the extreme values of stress intensity during the cycle.

in dry inert gas atmospheres compared to air,[2-5] and c) to be *decelerated* in dry hydrogen gas atmospheres in ultrahigh strength steels which are prone to hydrogen embrittlement.[4,6] To account for such surprising observations a new model for environmental effects, involving the role of excess corrosion debris generated within the crack in promoting crack closure, has recently been proposed for the near-threshold fatigue regime.[2,3] According to this model, termed *oxide-induced crack closure*,[2-5] near-threshold growth rates in lower strength steels are accelerated in dry, gaseous hydrogen because of an absence of moisture compared to air. Moist atmospheres result in the formation of readily observable oxide films within the crack,[2-9] which are thickened at low load ratios by "fretting oxidation",[9] *i.e.* a continual breaking and reforming of the oxide scale behind the crack tip due to a "smashing" together of crack surfaces as a result of plasticity-induced crack closure.[10] This oxide debris, which must be less pre-

dominant in dry, oxygen-free atmospheres or at high load ratios (where there is no plasticity-induced closure) provides a mechanism for increased crack closure. By resulting in an earlier contact between the fracture surfaces during the closing portion of the load cycle, closure loads are raised and the effective stress intensity range at the crack tip reduced, *i.e.* the presence of the oxide debris effectively raises K_{min}. This mechanism for environmentally-affected crack growth, however, is specific only to stress intensity ranges where oxide thicknesses are of the order of crack tip opening displacements (CTOD), *e.g.* at near-threshold levels.

The object of the present paper is to report new evidence supporting the concept of oxide-induced crack closure, and to comment on its significance to near-threshold corrosion fatigue in pressure vessel steels tested in air, water, hydrogen and helium atmospheres. In particular, a characterization of crack flank oxide deposits is made using ESCA and Auger spectroscopy. Further, additional contributions to enhanced crack closure at low stress intensities resulting from varying fracture surface morphology are discussed in the light of the mechanical, microstructural and environmental behavior patterns commonly observed at near-threshold levels.

EXPERIMENTAL PROCEDURES

The two pressure vessel steels investigated were both 2 ¼ Cr-1 Mo steels, namely ASTM A542 Classes 2 and 3 (hereafter referred to as SA542-2 and SA542-3 respectively), of composition shown in Table I. The SA542-2 steel, which was supplied as 25 mm thick plate, was fully martensitic following water quenching from 927 °C prior to tempering (1 ½ h) at 638 °C. The lower strength SA542-3 was supplied as 175 mm thick plate, and after water quenching from 954 °C and tempering (7 h) at 663 °C, the microstructure was found to be fully bainitic (<3 pct ferrite), uniformly through the thickness. A few additional tests were performed on SA542-2, reaustenitized at 950 °C, water quenched and tem-

S. SURESH is Research Assistant, Department of Mechanical Engineering, Massachusetts Institute of Technology, Cambridge, MA 02139. G. F. ZAMISKI, formerly with M.I.T., is with McDonnell-Douglas Corporation, Redondo Beach, CA. R. O. RITCHIE, formerly with M.I.T., is Associate Professor, Department of Materials Science and Mineral Engineering, and Lawrence Berkeley Laboratory, University of California, Berkeley, CA 94720.
Manuscript submitted December 17, 1980.

pered (1 h) at 690 °C, to give a lower strength martensitic structure (referred to as SA542-2/T690). Ambient temperature mechanical properties are listed in Table II.

Fatigue crack propagation experiments were performed with 12.7 mm thick compact specimens,* ma-

---

*Plane strain conditions were maintained, based on the criteria that cyclic plastic zone sizes did not exceed 1/15 of test-piece thickness.

---

chined in the T-L orientation between quarter and mid-thickness sections of the plates. Testing was performed on 50 kN Instron electro servo-hydraulic machines, operating under load control at 50 Hz (sine wave) at load ratios R of 0.05 and 0.75. Tests were conducted at ambient temperature in moist air (30 pct relative humidity), distilled water, and high purity dehumidified hydrogen and helium gases. Hydrogen and helium atmospheres were maintained at 138 kPa pressure in a small O-ring sealed chamber, clamped onto the test-piece, where gas purity was obtained using an extensive purification system, involving molecular sieves, cold traps, and heat bakeable lines. The system, which was modelled on procedures of Gangloff and Wei,[11] is described elsewhere.[12] Crack growth monitoring was achieved using DC electrical potential techniques capable of detecting changes in crack length of the order of 0.01 mm.[13]. Near-threshold growth rates (below 10^{-6} mm/cycle) were measured under both load-shedding (decreasing stress intensity) and increasing stress intensity conditions, with the threshold ΔK_o defined in terms of a maximum growth rate of 10^{-8} mm/cycle.[8] Growth rates above 10^{-6} mm/cycles were measured at constant load amplitude. Full experimental details have been described elsewhere.[2,12-16]

Characterization of corrosion deposits on fatigue fracture surfaces was performed using a fully computer-controlled ESCA/Scanning Auger spectrometer. ESCA (X-ray Photoelectron Spectroscopy) studies were conducted on fracture surfaces at 25Å depth (after ion sputter-etching). By comparing the resulting ESCA survey spectra with standard spectra, the compositon of

the fracture surface oxide was deduced. To determine the extent of oxidation, depth-composition profiles were obtained on broken fracture surfaces as a function of Auger sputtering time. Using a beam voltage of 5 kV, ion and electron beam sizes of roughly 200 and 25 μm respectively, and rastering rates of 180 Hz (x-direction) and 30 Hz (y-direction), sputter time was calibrated using a known thickness of tantalum oxide standard.* O

---

*Background oxide thicknesses on fracture surfaces were found to be 50 to 150Å. Since this was of the order of the thickness of natural oxide formed on metallographically polished samples simply exposed to the same laboratory air environment for similar times, oxide growth during the transfer of fracture surfaces to the Auger spectrometer was considered negligible.

---

and Fe, as well as C, profiles were monitored at a sputter rate of approximately 100Å/min. From this information, the thickness of fracture surface oxide debris was estimated as a function of crack length.

RESULTS

For the bainitic SA542-3 steel tested at $R = 0.05$ and 0.75, the variation of fatigue crack propagation rate (da/dN) at 50 Hz with alternating stress intensity ($\Delta K = K_{max} - K_{min}$) is illustrated in Fig. 1. Above 10^{-6} mm/cycle, crack growth data in dry hydrogen and moist air at both load ratios are similar, whereas near-threshold propagation rates in hydrogen exceed those in air by up to two orders of magnitude at $R = 0.05$, with threshold ΔK_o values 48 pct higher in air.*

---

*Hydrogen-assisted fatigue crack growth is observed in this steel above 10^{-5} mm/cycle, but only at lower frequencies (<5Hz) when K_{max} exceeds ~20 MPa $\sqrt{m}$, but is accompanied by a transition to predominately intergranular fracture[4,15].

Little difference, however, is apparent at $R = 0.75$. In dry helium gas at $R = 0.05$ (Fig. 2), growth rates above 10^{-6} mm/cycle are lowered compared to air, although below 10^{-6} mm/cycle the presence of the inert gas actually *accelerates* near-threshold growth compared to air by over an order of magnitude, with threshold ΔK_o values 24 pct higher in air. A distilled water environment, conversely, results in a marginal *retardation* in near-threshold growth, with a threshold ΔK_o value fractionally above that measured in air (Fig. 2).

Similar results are seen in the higher strength martensitic SA542-2 steel and the reheat treated SA542-2/T690 steel tested in moist air and dry hydrogen and helium gases (Figs. 3 through 5). For the SA542-2 steel, near-threshold growth rates in hydrogen are significantly

Table I. Base Plate Chemistries of 2¼ Cr-1 Mo Steels (Wt. Pct)

	C	Mn	Si	Ni	Cr	Mo	P	S	Cu
SA542-2	0.14	0.44	0.22	0.61	2.28	0.92	0.010	0.020	—
SA542-3	0.12	0.45	0.21	0.11	2.28	1.05	0.014	0.015	0.12

Table II. Ambient Temperature Mechanical Properties of 2¼ Cr-1 Mo Steels (1/4T-1/2T sections)

Steel	Structure	Yield Strength*		UTS (MPa)	Reduction in Area (Pct)	K_{Ic} (MPa $\sqrt{m}$)	K_{Iscc}† (MPa $\sqrt{m}$)
		Monotonic (MPa)	cyclic (MPa)‡				
SA542-3	bainite	500	400	610	77	295	85
SA542-2	martensite	769	568	820	56	—	80
SA542-2/T690	martensite	575	460	697	65	—	—

*0.2 pct offset yield stress.
†Measured in 138 kPa dry gaseous hydrogen.
‡Measured using incremental step tests.

Fig. 1—Fatigue crack propagation in bainitic SA542-3 tested at $R = 0.05$ and 0.75 (50 Hz) in moist air and dry hydrogen, showing accelerated near-threshold growth rates in hydrogen only at $R = 0.05$.
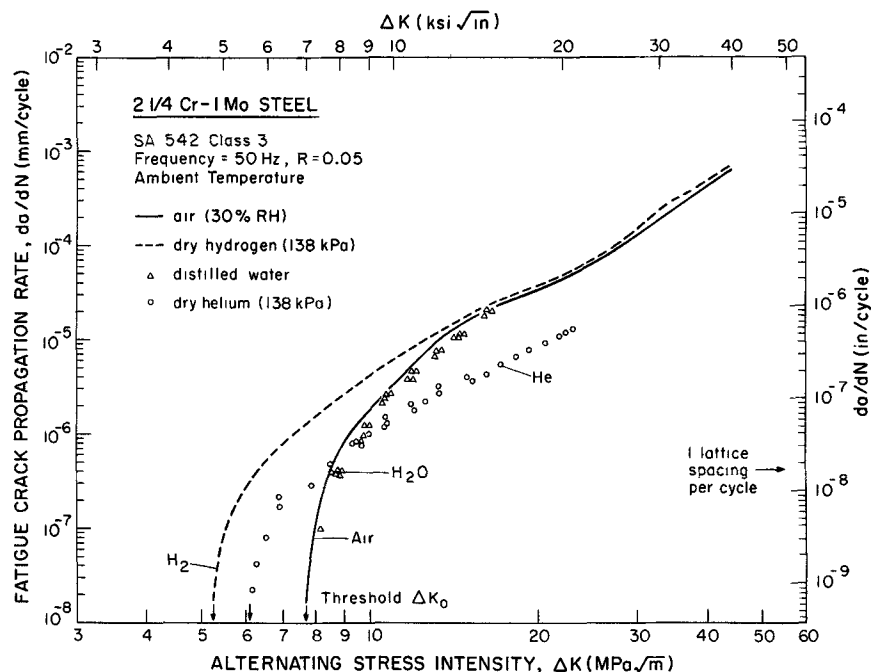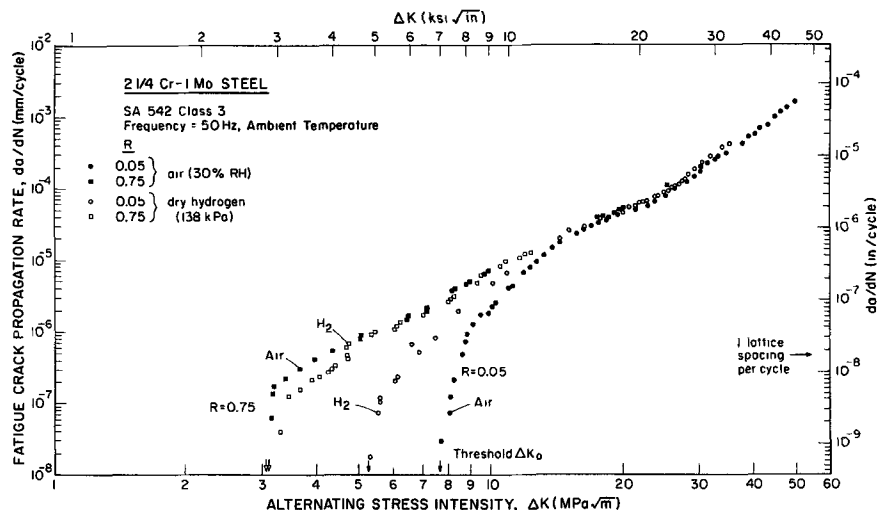

Fig. 2—Fatigue crack propagation in bainitic SA542-3 tested at $R = 0.05$ (50 Hz) showing influence of environment, namely moist air, water, and dry hydrogen and dry helium gases.

Table III. Threshold Data for 2¼ Cr-1 Mo Steels

Steel	Environment	R	ΔK_o (MPa $\sqrt{m}$)	CTOD* Cyclic (μm)	CTOD* Maximum (μm)	Maximum Oxide Thickness (μm)
SA542-3	moist air	0.05	7.7	0.18	0.31	0.20
($Y = 500$MPa)	moist air	0.75	3.2	0.03	0.78	0.01
	dry H_2	0.05	5.2	0.08	0.14	0.09
	dry H_2	0.75	3.3	0.03	0.83	0.01
	dry He	0.05	6.2	0.11	0.20	0.10
	water	0.05	7.8	0.18	0.32	0.25
SA542-2	moist air	0.05	7.1	0.11	0.17	0.12
($Y = 769$MPa)	moist air	0.75	2.8	0.02	0.41	—
	dry H_2	0.05	4.6	0.04	0.07	0.04
	dry H_2	0.75	2.8	0.02	0.38	—
	dry He	0.05	4.9	0.05	0.08	0.04
	dry He	0.75	2.7	0.02	0.35	—
SA542-2/T690	moist air	0.05	8.6	0.19	0.34	0.16
($Y = 575$MPa)	dry H_2	0.05	6.9	0.12	0.22	0.11
	dry He	0.05	7.1	0.13	0.23	0.11

*Plane strain values defined as 0.49 $(\Delta K_o^2/2Y'E)$—cyclic, and 0.49 $(K_{max,o}^2/YE)$—maximum, where ΔK_o and $K_{max,o}$ are the cyclic and maximum threshold stress intensities, Y' and Y are the cyclic and monotonic yield strengths and E is the elastic modulus.
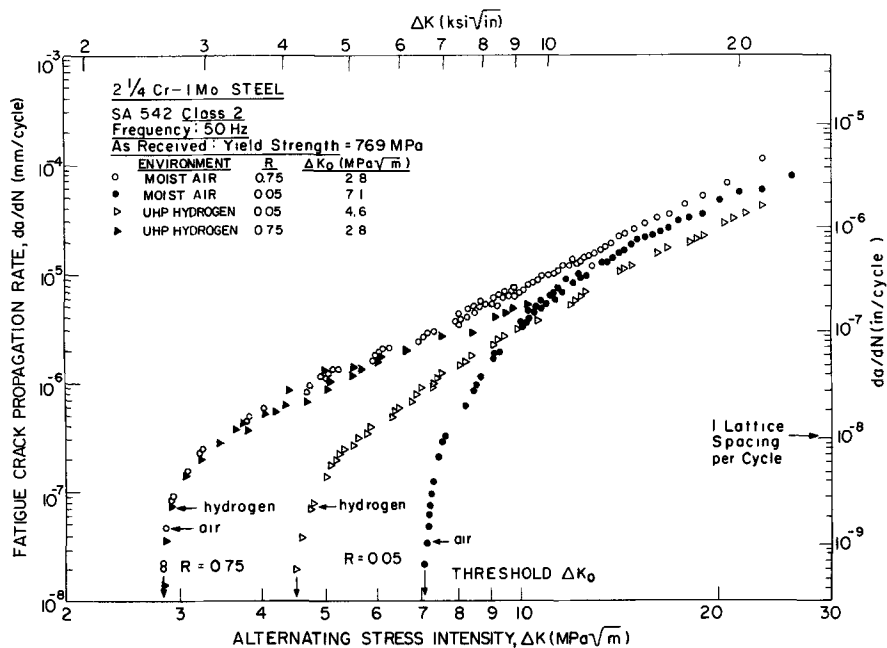
Fig. 3—Fatigue crack propagation in martensitic SA542-2 tested at $R = 0.05$ and 0.75 (50 Hz) in moist air and dry hydrogen gas.
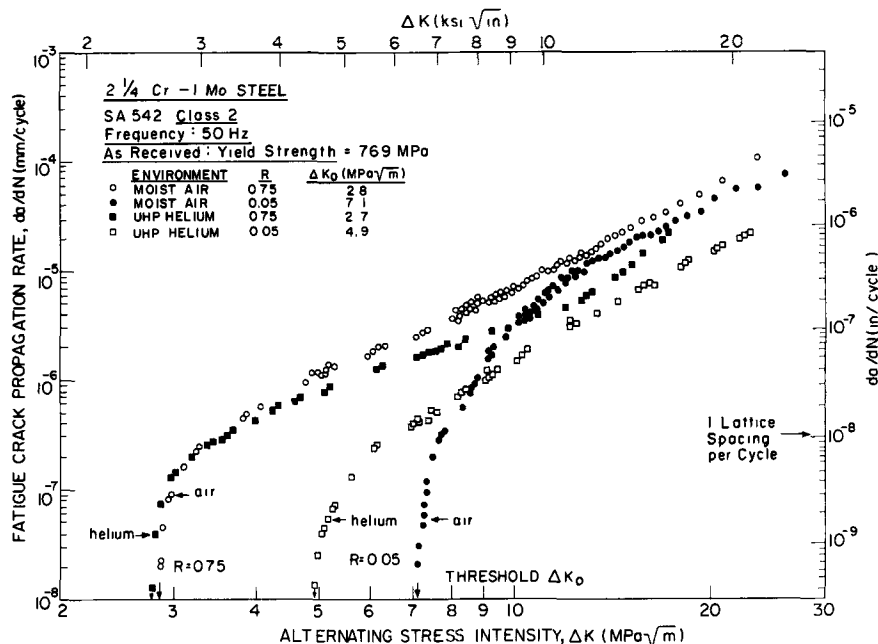

Fig. 4—Fatigue crack propagation in martensitic SA542-2 tested at $R = 0.05$ and 0.75 (50 Hz) in moist air and dry helium gas.

enhanced compared to air at $R = 0.05$ ($\Delta K_o \sim 54$ pct higher in air), with no effect of hydrogen again being observed at $R = 0.75$ (Fig. 3). Dry helium similarly accelerates near-threshold growth rates compared to air ($\Delta K_o \sim 45$ pct higher in air), but again only at low load ratios (Fig. 4). These threshold data (Table III), together with parallel results on normalized bainitic/ferritic 2¼ Cr-1 Mo steel (SA387),[2,16] are plotted in Fig. 6 as a function of yield strength. In addition to a general trend of decreasing threshold ΔK_o values with increasing strength in these steels,* it is apparent that both dry

---

* Similar effects of strength level on ΔK_o have been reported for a wide range of steels. See, for example, Refs. 8 and 14.

---

hydrogen and helium atmospheres significantly lower ΔK_o values compared to air at $R = 0.05$, whereas at R

$= 0.75$ environment has little influence on threshold behavior. Fractographically, failures in both Class 2 and Class 3 steels were similar. At near-threshold stress intensities, fracture morphology consisted of a fine-scale transgranular mode with evidence of additional intergranular separation (Fig. 7). The proportion of intergranular facets, which were not seen at $R = 0.75$, increased with increasing ΔK to a maximum of typically 30 to 40 pct at $\Delta K \sim 15$ MPa $\sqrt{m}$, before decreasing to zero above $\Delta K \sim 20$ to 25 MPa $\sqrt{m}$, in air, water, and hydrogen environments. Little evidence of such facets was seen in helium tests. Thus, the occurrence of intergranular facets near ΔK_o does not appear to directly correlate with subsequent growth rate behavior. At $R = 0.05$, near-threshold growth rates are similar in

Fig. 5—Fatigue crack propagation in martensitic (re-heat treated) SA542-2/T690 steel tested at $R = 0.05$ (50 Hz) in moist air, dry hydrogen and dry helium gases.
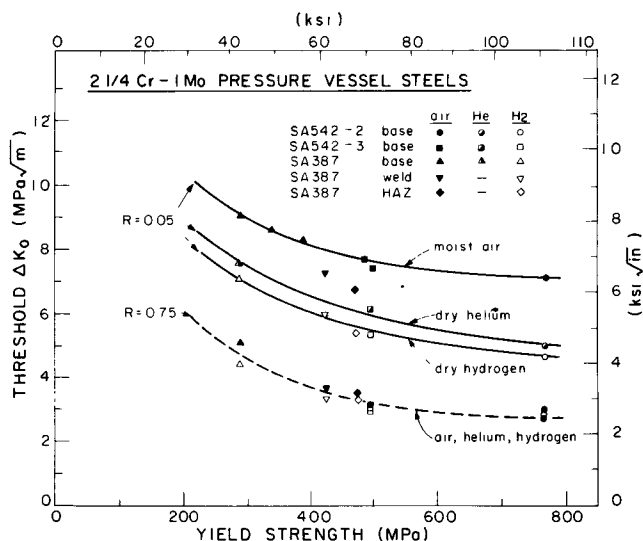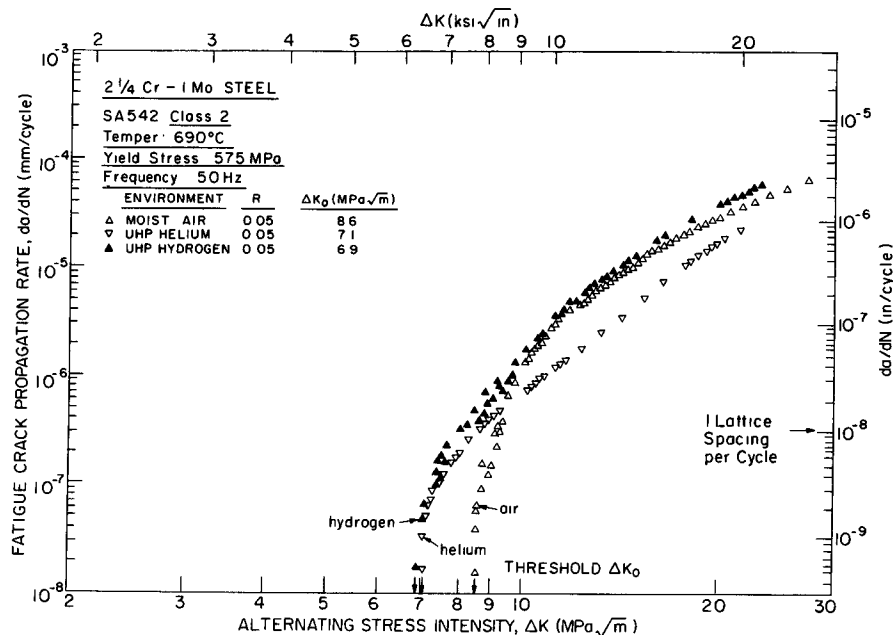

Fig. 6—Variation of threshold ΔK_o values for as-received $2\frac{1}{4}$ Cr-1 Mo pressure vessel steels with yield strength. Data for $R = 0.05$ and 0.75 in moist air, dry hydrogen and dry helium environments.

hydrogen and helium where the proportion of intergranular fracture is different, whereas proportions of intergranular fracture are similar in air and hydrogen where growth rates are very different.

Macroscopically, fracture surfaces in both steels were characterized by bands of corrosion deposits (Fig. 8), which were identified using ESCA to be predominately Fe_2O_3 (Fig. 9). The oxide, which appeared thickest in air and water tests, was not visible at high load ratios. Actual thickness measurements, as a function of crack length (and thus growth rate) are shown in Fig. 10 for SA542-3 steel, estimated using Ar^+ sputtering analysis in the Auger spectrometer. It is apparent that oxide thicknesses are inversely related to crack growth rate, and are at a maximum close to ΔK_o. In air, the maximum thickness is of the order of 0.2 μm at $R = 0.05$,

compared to less than 0.1 μm in hydrogen.* At R

* Presumably because of fretting mechanisms for enlarged oxide formation, it is apparent that even after extensive purification of the gaseous hydrogen, some oxide can form near the threshold at low load ratios, due to residual traces of moisture.

$= 0.75$, oxide thicknesses in either environment were an order of magnitude smaller. Note that since one unit volume of Fe produces 2.13 unit volumes of Fe_2O_3, the oxide thickness measurements shown in Fig. 10 represent approximately the total excess material inside the crack (assuming equal thickness on each crack face). Also note that these oxide thicknesses are comparable to pulsating crack tip opening displacements close to the threshold (Table III).

DISCUSSION

Previous studies in $2\frac{1}{4}$ Cr-1 Mo steels have shown that two distinct growth rate regimes exist where hydrogen markedly accelerates fatigue crack propagation compared to air (Fig. 11), namely a) at near-threshold levels, involving no change in fracture mode (predominately transgranular) and b) at higher growth rates (typically $>10^{-5}$ mm/cycle) above a critical K_{max} value (K_{max}^T) involving a fracture mode change to predominately intergranular cracking.[15,4] Environmentally-assisted growth in the latter regime, which is only observed below a critical frequency[15] (e.g. 5 Hz at $R = 0.05$), has been attributed to hydrogen embrittlement,[17] although precise micromechanisms of such embrittlement in these lower strength steels are unclear at this time. At near-threshold levels, however, hydrogen embrittlement theories to explain the observed environmentally-affected growth rate behavior must be questioned.[2-4] As shown in the present work, compared to moist air, dry hydrogen accelerates near-threshold growth rates only at low load ratios (Figs. 1, 3 and 5), water results in a marginal deceleration in growth rates
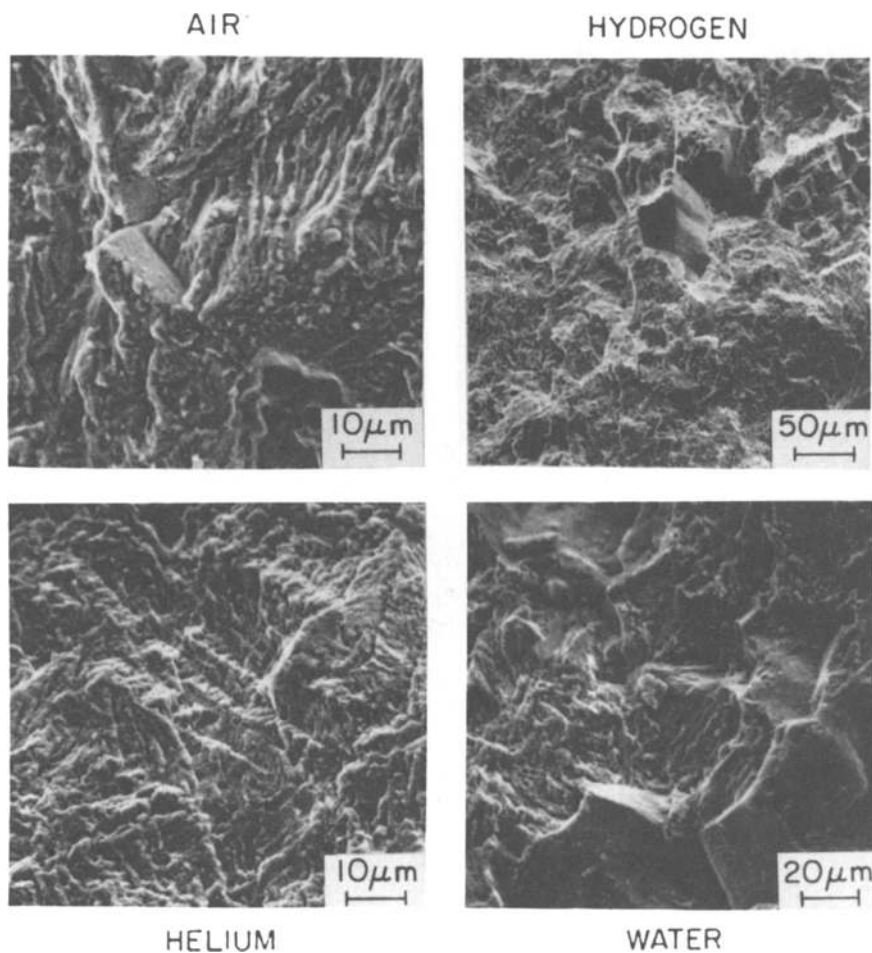
AIR

HYDROGEN

Fig. 7—Fractography of near-threshold fatigue crack growth in SA542-3 steel, tested in moist air, dry hydrogen, dry helium and distilled water.

HELIUM

WATER

$\Delta K_o = 7.7$ MPa$\sqrt{m}$ ⟶

⟵ $\Delta K_o = 3.1$ MPa$\sqrt{m}$
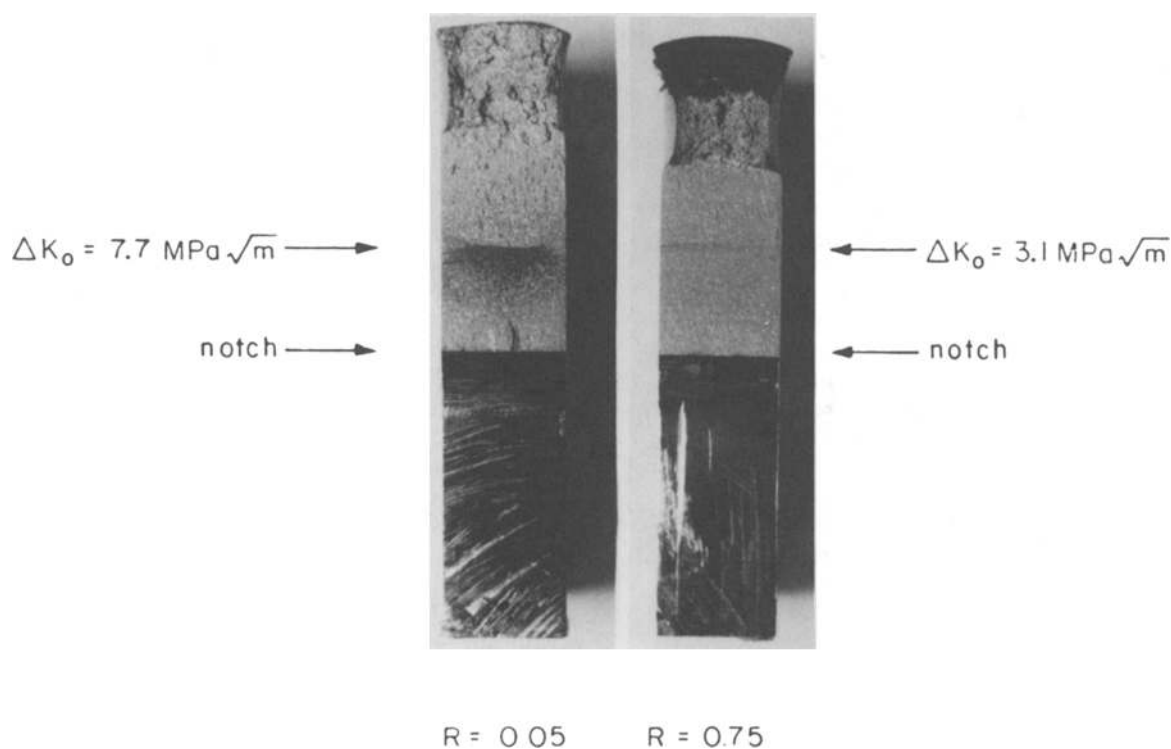
notch ⟶

⟵ notch

R = 0.05   R = 0.75

Fig. 8—Bands of corrosion deposits visible on near-threshold fatigue fracture surfaces of SA542-3 tested in moist air at (a) R = 0.05 and (b) R = 0.75.

(Fig. 2), dry helium gas results in a marked *acceleration* in near-threshold rates at $R = 0.05$ (Figs. 2, 4 and 5), and further there is no characteristic fracture mode for environmentally-assisted growth (Fig. 7). Such observations, however, are in accord with concepts of oxide-induced crack closure.[2,3]

During fatigue crack growth, material is plastically strained at the crack tip, and due to the restraint of
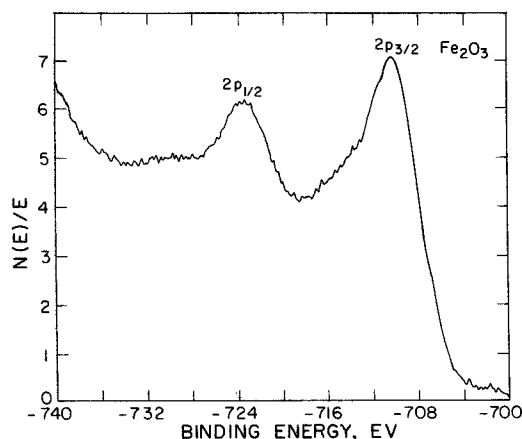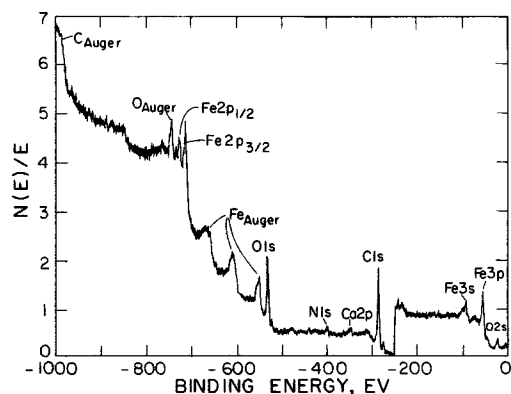

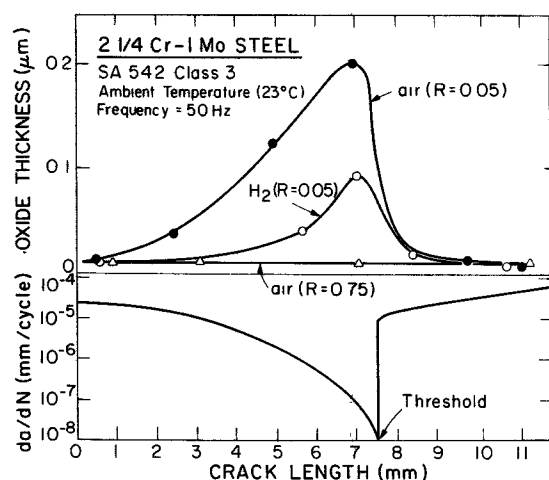Fig. 9—ESCA analysis of crack tip corrosion debris in SA542-3 showing presence of predominately Fe_2O_3.

Fig. 10—Measurements of oxide thickness as a function of crack length and crack growth rate (da/dN) for SA542-3 tested in air and hydrogen gas at $R = 0.05$ and 0.75. Data from Ar^+ sputtering analysis using Auger spectroscopy.
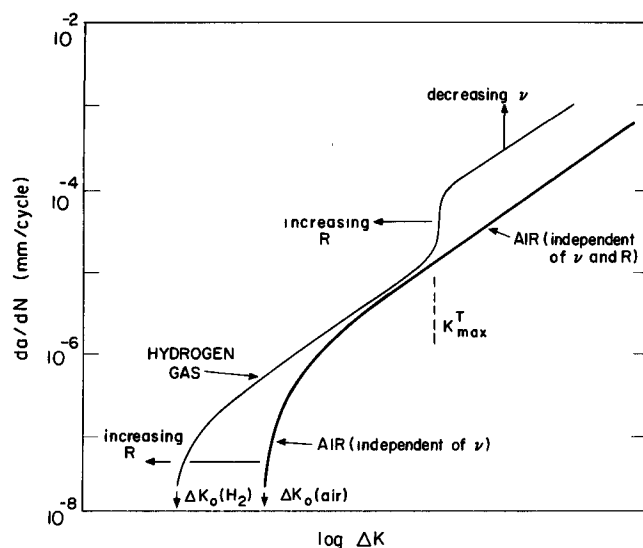

Fig. 11—Schematic diagram showing regimes of hydrogen-assisted growth commonly observed in lower strength steels. R is load ratio and v is frequency.

surrounding elastic material on this residual stretch, some closure of the crack surfaces may occur at positive loads during the loading cycle.[10] Since the crack cannot propagate while it remains closed, such "plasticity-induced closure" can result in a reduced ΔK value actually experienced at the crack tip, *i.e.* $\Delta K_{eff} = K_{max} - K_{cl}$, where K_{cl} is the stress intensity to close the crack. As the load ratio is increased, however, the crack remains open during a larger portion of the cycle and the role of crack closure becomes less significant (*i.e.* $\Delta K_{eff} \rightarrow \Delta K$). In oxidizing environments, where crack tip opening displacements are small, such closure provides a mechanism for enhanced corrosion debris formation within the crack by repeated breaking and compacting of the oxide (fretting oxidation).[9] In the present work, such oxide thicknesses generated in air environments are as large as 0.2 μm (Fig. 10 and Table III), over an order of magnitude larger than oxide formed on a freshly-exposed surface left in the same environment for the same length of time. At high load ratios, where plasticity-induced closure and hence fretting oxidation mechanisms are absent, no such enlarged oxide deposits are generated (Figs. 8 through 10.) The consequence of this excess debris formed within the crack is that, where crack tip opening displacements are small, *i.e.* at near-threshold levels, its presence will lead to earlier contact between crack surfaces, thereby raising K_{cl} and thus reducing the effective ΔK. In fact, with respect to the current data (Table III), it appears that the threshold ΔK_o for no crack growth is consistent with a maximum oxide thickness of the order of the pulsating crack tip opening displacement. Such a result is clearly physically appealing since it infers that the crack will be "wedged closed" at the threshold such that ΔK_{eff} has no finite value.

The role of environment in influencing *near-threshold* fatigue crack growth can thus be readily explained. Crack growth rates in dry hydrogen at $R = 0.05$ exceed those in air because limited oxide formation results in lower K_{cl} values and hence larger effective stress

intensities. Any dry, reducing or inert environment should behave similarly, as indicated by results at low ratios in helium (and argon[2]). At $R = 0.75$, where plasticity-induced closure and hence enhanced oxide formation is insignificant, crack growth rates in air, hydrogen and helium are identical. In moist oxidizing environments, such as air and water, near-threshold growth rates at low R are significantly lower simply due to enhanced oxide-induced closure. As described elsewhere,[2] the marked effect of load ratio, which is specific to the near-threshold regime, is also consistent with this model.

The idea of corrosion deposits forming in cracks and influencing subsequent growth behavior is not entirely new. Swanson and Marcus,[18] for example, have observed enhanced oxygen transport into the matrix during fatigue crack growth of several non-ferrous metals tested in oxygen environments. Tu and Seth[19] report slower near-threshold growth rates in several rotor steels tested at 100 °C in the seemingly more aggressive environment of steam compared to air; a fact they attribute to a number of factors including crack-tip corrosion deposits. Nordmark and Fricke[20] use a similar argument to explain crack arrest during fatigue of 7475 aluminum alloys in sump water. Skelton and Haigh[21] interpret their results of lowered ΔK_o values *in vacuo* and at $R = -1$ in Cr-Mo-V steels at 550 °C in terms of reduced crack tip displacements from "shear lips and oxide filling" of the crack. In addition,the hitherto unexplained result of Paris *et al*[22] where near-threshold fatigue crack growth in nuclear pressure vessels steels was retarded by adding water is clearly consistent with the idea of oxide-induced crack closure.

Many aspects of the phenomenon of oxide-induced crack closure remain unexplored. For example, effects of alloy composition, microstructure, temperature, pressure, and so forth, on oxide debris size and associated closure have not been resolved. Further, mechanisms for enhanced oxide growth within cracks, such as fretting oxidation,[9] are still somewhat vague. In this light, recent studies in mild steels by Davidson[23] have identified a strong Mode II component at low load ratios in crack growth mechanisms very close to ΔK_o. Such a sliding component, which would be essential to any fretting mechanism and hence perhaps to enhanced oxide formation, was found to be delayed to lower ΔK levels in gaseous hydrogen and to be almost non-existent at high R. These observations are clearly consistent with the present oxide measurements (Fig. 10), and furthermore may provide the clue as to why thick oxide deposits only occur close to ΔK_o.

CONCLUDING REMARKS

The current studies have shown how, inside near-threshold cracks were pulsating crack tip displacements are small, the presence of foreign debris can have a profound influence on subsequent crack growth behavior through mechanisms of crack closure. However, since the size-scale of the fracture morphology may also be of comparable size, it is interesting to speculate on additional sources of closure from fracture surface roughness[24] and irregular morphology.[25] Given the pres-

ence of a Mode II component at near-threshold levels, a rougher fracture surface clearly implies enhanced closure loads by wedging open the crack at discrete contact points along crack faces.[25] One can now envisage possible explanations, not only for the strong environmental and load ratio effects near ΔK_o, but also for the marked influences of yield strength[8,14,26-28] and grain size[8,28-32] which are specific to the near-threshold regime. The role of increased strength in decreasing ΔK_o values may simply result from reduced crack closure, arising from limited plasticity-induced closure,[5] less fretting[3-5] or perhaps smoother fracture surfaces.[24] Certainly higher strength steels show far less retardation in crack growth following single positive overload cycles,[33] a phenomenon often explained in terms of crack closure arguments. The role of finer grain size in similarly decreasing ΔK_o values again may simply be a result of reduced crack closure from less fracture surface roughness. Such an explanation is more appealing than those based on inherent microstructural reasons where plastic zone sizes near ΔK_o are often far less than a grain diameter. Quantitative verification of these ideas is in most instances lacking, but it is interesting to note that, similar to the role of moist environments seen in the present work, the beneficial effects of lower strength and coarser microstructures in reducing near-threshold growth rates are generally far less evident, and often non-existent, at high load ratios,[8,14,26-28] an observation which strongly suggests a prominent role of crack closure.

In summary, it is clear that concepts of crack closure are of paramount importance to fatigue crack growth behavior *at near-threshold levels,* although the mechanisms of such closure may be very different from the plasticity-induced closure originally proposed by Elber.[10] At low stress intensities, closure mechanisms originate from the fact that pulsating crack tip opening displacements are of a size comparable with fracture surface roughness and the thickness of corrosion debris within the crack. These ideas, although still somewhat speculative at this time, suggest a very different role of alloy composition and microstructure in influencing fatigue cracking, a role which may have a profound influence on the direction which should be taken for the design of alloys with increased resistance to fatigue crack propagation at ultralow growth rates.

CONCLUSIONS

Based on a study of ambient temperature corrosion fatigue crack propagation in bainitic and martensitic 2 ¼ Cr-1 Mo pressure vessels steels (SA542-2 and SA542-3) the following conclusions can be made:

1) Fatigue crack propagation above 10^{-5} mm/cycle was largely independent of load ratio, strength level and environment for tests at 50 Hz in moist air, water and dry gaseous hydrogen. Growth rates in dry helium in this regime were nearly an order of magnitude lower.

2) At near-threshold levels, below 10^{-6} mm/cycle, growth rates in dry gaseous hydrogen exceeded those in moist air by up to two orders of magnitude, with ΔK_o values approximately 40 pct higher in air. The accelerating effect of hydrogen, however, was only apparent

at $R = 0.05$; at $R = 0.75$ growth rates and ΔK_o values were identical in air and hydrogen.

3) Near-threshold growth rates in dry gaseous helium at $R = 0.05$ were similarly *accelerated* with respect to air by over an order of magnitude with ΔK_o values 24 to 45 pct higher in air. At high load ratios ($R = 0.75$) growth rates and ΔK_o values in helium were identical to those measured in air and hydrogen.

4) In SA542-3, near-threshold growth in distilled water at $R = 0.05$ were marginally slower than those measured in air, with ΔK_o values fractionally above the air value.

5) Fractographically, fracture surfaces consisted of a fine-scale transgranular mechanism with additional intergranular facets. The maximum proportion of such intergranular fracture (~ 30 to 40 pct) was observed at $\Delta K \sim 15 - 20$ MPa $\sqrt{m}$ in air and hydrogen atmospheres at $R = 0.05$. Little evidence of such fracture was found at $R = 0.75$ or for tests in helium. The presence of intergranular facets did not appear to directly influence near-threshold growth rate behavior.

6) Macroscopically, bands of corrosion deposits, identified as predominately Fe_2O_3, were observed on fracture surfaces. The thickness of the oxide, which was inversely related to growth rate, was at a maximum at the threshold. Oxide thicknesses were significantly smaller in hydrogen gas compared to air at $R = 0.05$, and were an order of magnitude smaller in either environment at $R = 0.75$. Such thicknesses were significantly greater than those obtained by simply exposing the same material in the same environment for the same length of time.

7) The influence of environment on *near-threshold* fatigue crack growth is ascribed to a new mechanism involving oxide-induced crack closure. According to this model, near-threshold growth rates are accelerated in inert or reducing atmospheres (*i.e.* H_2, He) because the environment contains less moisture (and oxygen) compared to air. Moist environments result in oxide films formed at the crack tip, which are thickened by fretting oxidation arising from plasticity-induced crack closure. Since the excess oxide debris is of comparable size to crack tip opening displacements, a source of enhanced crack closure is realized thereby reducing effective ΔK values at the crack tip.

8) Based on limited data it appears that at the threshold stress intensity ΔK_o, the maximum excess oxide thickness is of the order of the pulsating crack tip opening displacement.

9) In addition to mechanisms generated by corrosion debris, sources of enhanced crack closure from fracture surface morphology and roughness are significant at near-threshold levels because their size-scales are comparable to crack tip displacements. Such concepts are consistent with experimental observations of the influence of load ratio, strength, grain size and environment on near-threshold growth.

ACKNOWLEDGMENTS

REFERENCES

1. For example, see *Proceedings of Intl. Conf. on Corrosion Fatigue, Chemistry, Mechanics, Microstructure, Storrs, Connecticut*, Nat. Assoc. Corrosion Engineers, 1971.
2. R. O. Ritchie, S. Suresh, and C. M. Moss: *J. Eng. Mater. Technol., Trans. ASME Series H*, 1980, vol. 102, p. 293.
3. A. T. Stewart: *Eng. Fract. Mech.*, 1980, vol. 13, p. 463.
4. R. O. Ritchie: *Analytical and Experimental Fracture Mechanics*, G. C. Sih, and M. Mirabile, eds., Sijthoff and Noordhoff, 1981.
5. S. Suresh, G. F. Zamiski, and R. O. Ritchie: *The Application of 2¼ Cr-1 Mo Pressure Vessel Steel for Thick-Wall Pressure Vessels*, ASTM STP 755, 1981.
6. J. Toplosky: S. M. Thesis, Dept. of Mech. Eng., M.I.T., 1981.
7. R. J. Cooke and C. J. Beevers: *Mater. Sci. Eng.*, 1974, vol. 13, p. 201.
8. R. O. Ritchie: *Int. Metall. Rev.*, 1979, vol. 20, p. 205.
9. D. Benoit, R. Namdar-Tixier, and R. Tixier: *Mater. Sci. Eng.*, 1981, vol. 45, p. 1.
10. W. Elber: ASTM STP 486, p. 280, 1971.
11. R. P. Gangloff and R. P. Wei: *Metall. Trans. A.*, 1977, vol. 8A, p. 1043.
12. G. F. Zamiski: S. M. Thesis, Dept. of Mech. Eng., M.I.T., July 1980.
13. R. O. Ritchie: *Crack Growth Monitoring: Some Considerations on the Electrical Potential Method*, Dept. of Metallurgy and Materials Science Technical Report, Cambridge University, Jan. 1972.
14. R. O. Ritchie: *J. Eng. Mater. Technol., Trans. ASME Series H*, 1977, vol. 99, p. 195.
15. S. Suresh, C. M. Moss, and R. O. Ritchie: *Trans. Jpn. Inst. Met.*, 1980, vol. 21, p. 481.
16. R. O. Ritchie and R. Fuquen-Molano: M.I.T. Fatigue and Plasticity Laboratory Report No. FPL/R/80/1035, Oct. 1980.
17. R. L. Brazill, G. W. Simmons, and R. P. Wei: *J. Eng. Mater. Technol.*, Trans. ASME, Series H, 1979, vol. 101, p. 199.
18. J. W. Swanson and H. L. Marcus: *Metall. Trans. A.*, 1978, vol. 9A, p. 291.
19. L.K.L. Tu and B. B. Seth: *J. Test Eval.*, 1978, vol. 6, p. 66.
20. G. E. Nordmark and W. G. Fricke: *ibid.*, p. 301.
21. R. P. Skelton and J. R. Haigh: *Mater. Sci. Eng.*, 1978, vol. 36, p. 17.
22. P. C. Paris, R. J. Bucci, E. T. Wessel, W. G. Clark, and T. R. Mager: ASTM STP 513, 1972, p. 141.
23. D. L. Davidson: *Fat. Eng. Mat. Struct.*, 1981, vol. 3, p. 229.
24. I. C. Mayes, and T. J. Baker: *Micromechanisms of Crack Extension*, Proc. Conf. on Mechanics and Physics of Fracture II, Metals Society/Institute of Physics, 1981, in press.
25. N. Walker and C. J. Beevers: *Fat. Eng. Mat. Struct.*, 1979, vol. 1, p. 135.
26. T. C. Lindley and C. E. Richards: Central Electricity Generating Board Note No. RD/L/N 135/78, Aug. 1978, CERL, U.K.
27. O. Vosikovsky: *Eng. Fract. Mech.*, 1979, vol. 11, p. 959.
28. R. O. Ritchie: *Met. Sci.*, 1977, vol. 11, p. 368.
29. J. Masounave and J.-P. Baïlon: *Scr. Metall.*, 1976, vol. 10, p.165.
30. C. J. Beevers: *Met. Sci.*, 1977, vol. 11, p. 362.
31. G. R. Yoder, L. A. Cooley, and T. W. Crooker: *J. Eng. Mater. Technol.*, Trans. ASME, Series H, 1979, vol. 101, p. 86.
32. W. W. Gerberich and N. R. Moody: ASTM STP 675, 1979, p. 292.
33. G. J. Petrak and J. P. Gallagher: *J. Eng. Mater. Technol.*, Trans. ASME, Series H, 1975, vol. 97, p. 206.